# Dynamics of Polymer Chain Pull-Out

**B. Lin[1] and P. L. Taylor***

*Department of Physics, Case Western Reserve University, Cleveland, Ohio 44106-7079*

*Received January 1, 1994; Revised Manuscript Received May 5, 1994*[⊕]

ABSTRACT: We propose a new one-dimensional microscopic model of polymer chain pull-out processes and perform computer simulation studies of this model. The dynamics of the pull-out process are found to be similar to the stick–slip dynamics observed in some models of earthquake motion. Chain pull-out may be thought of as an example of self-organized critical behavior, similar to that observed in avalanches in a growing pile of sand. The distribution of magnitudes of stick–slip events was found to follow a scaling relationship that was independent of some of the model parameters but changed with the level of dissipation and with the stiffness of the chain. The calculated fracture energy per chain was found to increase linearly with the crack speed when that speed is not too large, in agreement with some experiments. The dependence of fracture energy on the chain length, the chain stiffness, and the roughness of interface between the chain and the matrix was also studied and interpreted in terms of the dynamic behavior of the model.

## 1. Introduction

The adhesion between polymers has been a subject of great interest both in theory and in practice. Since different homopolymers are generally highly immiscible and the interface between them is very sharp, with few entanglements, the adhesion between two immiscible polymers is typically weak. Adding diblock copolymers to the interface between two different homopolymers to reinforce the adhesion is a technique that has been widely used and extensively studied.[2-13] Normally an A–B diblock copolymer is added to the interface between A and B homopolymers so that each block is miscible with one of the homopolymers. This reduces the interfacial tension, increases the interfacial width, and improves the adhesion. This improvement comes from the entanglement of the block copolymers on both sides of the interface and the formation of stitches between the two homopolymers through which stress acting on the interface can be transferred. The fracture toughness (i.e., the energy necessary to separate completely the two bulk homopolymers) is thus increased.

It is believed that the type of mechanism responsible for the failure of an interface reinforced by diblock copolymers depends on the degree of polymerization, the areal density of the copolymers, and the time scale on which the deformation occurs.[3-5] If the degree of polymerization of one or both copolymer chains is less than the average degree of polymerization between entanglements of the corresponding homopolymers and the time scale is sufficiently long, the failure mechanism of the interface is chain pull-out from the shorter-chain side of diblock copolymer chains, and the only energy-consuming source is the dissipation energy from the viscous pull-out processes.[3,4] When the polymerization indices of both block copolymer chains are greater than the average polymerization indices between entanglements of the corresponding homopolymers and the time scale is sufficiently short, then the interface fracture occurs by chain breaking, and this normally results in stronger interface reinforcement.[3-5] In this latter case, the interface fracture mechanisms can be further classified into pure chain scission and the formation and breakdown of crazes, depending on whether the areal density of the chains is lower or higher than some critical value. It was also recently pointed out[5] that the fracture mechanism can also be chain pull-out when the polymerization indices of the block copolymers are moderately high but the areal density of the chains is low.

We are interested in this paper in the fracture mechanism where polymer chains of one of the diblock copolymers are pulled out from the corresponding homopolymer matrix. In previous studies of polymer chain pull-out, the detailed dynamics of the pull-out process does not appear to have been given a great deal of attention either in theory or in experiment. We propose to rectify this on the theoretical side by building a one-dimensional microscopic model to investigate the chain pull-out problem, the motivation for this work being that such a model could provide information useful in understanding fracture mechanisms and the improvement of interface toughness by diblock copolymer chains. First we review some theoretical and experimental results for fracture energy in chain pull-out and for the stick–slip dynamics to which our model will be related.

There have been several models concerning the fracture energy $G$ for chain pull-out.[10-13] They all predict there to be a crack propagation speed $V^*$ above which the fracture energy increases linearly with the crack speed $V$ and below which $G$ is a constant. This constant is approximately equal to the critical energy $G_c$ (or $G_0$ in some literature) for the fracture to be initiated at the smallest of crack speeds. We thus have

$$G \approx \begin{cases} G_c & (V < V^*) \\ CV & (V > V^*) \end{cases} \tag{1}$$

where $C$ is a constant independent of $V$. The critical speed $V^*$ varies as $(\Sigma N)^{-1}$ in one model[10,11] with $\Sigma$ the areal density and $N$ the length of polymer chains.[2,11] The critical fracture energy $G_c$ is the minimal energy required to break the interface with crack speed $V \to 0$. Both linear and quadratic dependences of $G_c$ on N have been predicted,

$$G_c \propto \begin{cases} N\Sigma & \text{(refs 10 and 11)} \\ N^2\Sigma & \text{(ref 12)} \end{cases} \tag{2}$$

On the experimental side, the linear dependence of $G$ on $V$ has been observed.[2] The critical speed $V^*$, however, has not been reported in experiments. In addition, experiments also show a saturation of $G$ as $V$ increases beyond some critical value, and this is not predicted by theory. The relationship between the critical energy $G_c$ and the chain length $N$ and density $\Sigma$ has been studied in several systems.[2-5,7-9] It is found that $G_c$ increases with

⊕ Abstract published in *Advance ACS Abstracts*, June 1, 1994.

0024-9297/94/2227-4212$04.50/0 

$\Sigma$ and then saturates at large $\Sigma$ in the system where a thin layer of a polystyrene (PS)–polyisoprene (PI) diblock copolymer is added to the interface of PS and PI homopolymers.[2] In a system consisting of a poly(2-vinylpyridine) (PVP)–PS diblock copolymer at the interface of PVP and PS,[3] a linear relationship between $G_c$ and $\Sigma$ was observed and a saturation plateau was also observed. Data on the dependence of $G_c$ on $N$ were too scattered to obtain a definite relationship, with some data showing $G \sim N^2$ and some $G \sim N^\beta$ with $1 < \beta < 2$.

The details of stick–slip motion have been seen in many dynamic experiments performed on a macroscopic scale[14-16] and in many theoretical models.[17-22] In these systems, an external force pulls with constant speed and different parts of the system show time-dependent sticking or slipping motions, with the sizes and velocities of slipping motions spanning a wide range of magnitudes. This type of stick–slip dynamics, in which a wide range of event sizes occurs for general values of system parameters, may relate to the concept of self-organized criticality.[23] A simple deterministic spring–block model has been proposed by Burridge and Knopoff[17] and studied by many authors[18-22] in various versions. In many spring–block models,[17,19-21] the mechanism for the stick–slip dynamics is a frictional force whose strength becomes weaker as the velocity increases. In a recent paper, Vallette and Gollub[16] conducted an experiment on a rubber sheet, in which they observed a broad distribution of slipping event size, similar to what was observed in the above-mentioned spring–block models. However, they found the friction to be velocity strengthening rather than to be of the velocity-weakening form used in some models. This suggested that there is another class of stick–slip dynamics whose mechanism of instability is not velocity-weakening friction.

We have developed a one-dimensional spring–block model[22] that contains no frictional force other than a velocity-strengthening viscous force to dissipate energy. A random Gaussian potential acting on blocks was the source of instability of the system. We have observed self-organized critical behavior in the model and have calculated some dynamic quantities. In this paper we modify our previous system to give a microscopic model for the chain pull-out problem. We will calculate the time and space distributions of the slipping events and the event probability distribution and investigate the dependence of the dynamics on system size and pulling speed. We then will calculate the fracture energy and its dependence on the length and elastic parameters of the chain, roughness of the interface between the chain and the matrix, the level of viscous dissipation during the chain pull-out, and the pulling speed. An attempt will be made to explain the dependence of the fracture energy on some parameters by the effects of these parameters on the dynamic behavior. We do not attempt to relate the magnitudes of the predicted quantities to those of any particular polymers but rather seek to determine the scaling properties of the fracture energy.

## 2. Chain Pull-Out Model

We propose a one-dimensional model to simulate polymer chain pull-out from a glassy matrix. As sketched in Figure 1, $N$ particles representing monomers are connected into a chain by harmonic springs having spring constant (i.e., stiffness parameter) $s_1$. Each monomer in the chain will be acted on by a potential energy due to the presence of the neighboring chains. These potentials arise from the van der Waals and electrostatic forces acting between monomers and will depend on the position of a given monomer in relation to the positions of those on nearby chains. Because the glassy matrix in which the chain is embedded is assumed to be amorphous, there will be a strong random element in this potential energy of interaction. We accordingly represent the interchain forces by a nondissipative random Gaussian potential,

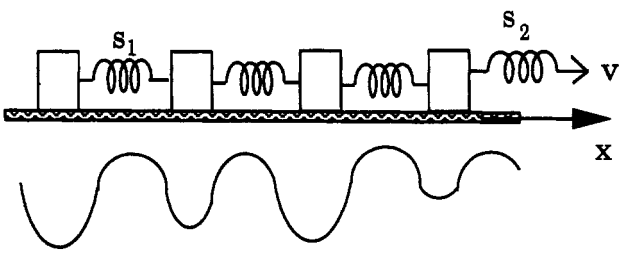


**Figure 1.** Mechanical model for one-dimensional chain pull-out.

$$U(x) = -\frac{k}{2d}\sum_i R_i e^{-d(x-i)^2} \tag{3}$$

where the integer $i$ is the index describing the position of a monomer in the polymer chain. The parameter $k$ describes the strength of the interaction between monomers on the chain and the surrounding matrix and reflects the difficulty in pulling a monomer out of the potential well caused by attractive forces and steric repulsions. It would be comparatively small for a monomer in poly(tetrafluoroethylene), which is close to cylindrical in shape when represented as a space-filling molecular model; for a styrene monomer, on the other hand, it would be larger. The quantity $d$ governs the width of the potential well and does not significantly affect the dynamic behavior as long as it is sufficiently large. We chose to set $d = 50$ in our calculations. The quantity $R_i$ is a random number between 0 and 1. This randomness accounts for the fact that entanglements and regions of locally high and low density occur in a random way as one proceeds along the polymer chain that is being pulled out of the matrix.

If we studied a model in which the potential $U(x)$ and the pull-out force were the only forces acting, we should find that the work done by the pulling force would raise the temperature of the chain to an unreasonable degree. It is thus necessary to introduce a dissipative component to the equation of motion. Most models do this by introducing a segmental friction coefficient. This would be inconsistent in our model, since the spatial irregularity of the potential $U$ is itself a microscopic description of a rough surface, and so friction has already been included. In fact, a significant advance made in our model is that we avoid such phenomenological approximations. On a microscopic level, the missing ingredient in our model is the fact that the monomers of the matrix will recoil when struck by a monomer in the chain being pulled. This recoil absorbs energy and prevents runaway heating of the chain. While it would be possible to include this effect by allowing some recoil motion in $U(x)$, we here take the simpler approach of retreating to phenomenology by including a small viscous force into the problem. We add a term $-\gamma(dx_i/dt)$ to the equations of motion for each monomer in the chain. We also include the pulling force by attaching to one end of the chain a spring of spring constant $s_2$, the other end of which is pulled at a steady speed $v$ in the $x$ direction.

The equations of motion for the general problem can then be written as

$$m\frac{d^2x_i}{dt^2} = s_1(x_{i+1} - 2x_i + x_{i-1}) + s_2[vt - (x_i - i)] - k\sum_{l=-\infty}^{+\infty} R_l(x_i - l)e^{-d(x_i-l)^2} - \gamma\frac{dx_i}{dt}, \quad i = 1, 2, \cdots, N \quad (4)$$

Since the chain is pulled at one end, the $s_2$ term should appear only in the equation for $x_N$. Furthermore, the viscous force $-\gamma(dx_i/dt)$ and that due to the random potential should vanish once the particle is pulled out of the matrix. The equations of motion for this model system are then rewritten as

$$\begin{aligned}
d^2x_N/dt^2 &= s_1(x_{N-1} + 1 - x_N) + s_2[vt - (x_N - N)] - f(x_N,\dot{x}_N)\\
d^2x_{N-1}/dt^2 &= s_1(x_N - 2x_{N-1} + x_{N-2}) - f(x_{N-1},\dot{x}_{N-1})\\
&\vdots\\
d^2x_i/dt^2 &= s_1(x_{i+1} - 2x_i + 2x_{i-1}) - f(x_i,\dot{x}_i), \quad i = N-2, N-3, \cdots, 2\\
&\vdots\\
d^2x_1/dt^2 &= s_1(x_2 + 1 - x_1) - f(x_1,\dot{x}_1)
\end{aligned} \quad (5)$$

where

$$f(x_i,\dot{x}_i) = \begin{cases} k\sum_l R_l(x_i - l)e^{-d(x_i-l)^2} + \gamma\dot{x}_i & \text{if } x_i \text{ is inside the matrix} \\ 0 & \text{otherwise} \end{cases} \quad (6)$$

We have taken the mass $m$ and the equilibrium interparticle spacing to be unity. We will use as an initial configuration of particles both a uniform distribution

$$x_i = i \quad (7)$$

and a spatially nonuniform configuration, with each particle deviating randomly by a small amount from its equilibrium position, so that

$$x_i = i + (\tilde{R}_i - 0.5)\delta \quad (8)$$

Here $\delta$ is a small constant and $\tilde{R}_i$ a random number in (0,1). Both sets of initial conditions are used to verify that no difference in dynamics and fracture energy results from the choice of initial configurations.

There are several one-dimensional spring–block earthquake models[17-22] which bear some similarities to our model (5). In Burridge and Knopoff's earthquake model[17] and its variants,[19,20] blocks are similarly connected by harmonic springs, but each block is pulled at the same speed. They used a velocity-weakening frictional force between blocks and the surface to generate instability so that the system showed large-scale fluctuations of stick–slip dynamics similar to the behavior observed in some self-organized critical systems. While velocity-weakening friction can describe some properties of an earthquake's stick–slip dynamics, there are some physical systems that do not have velocity-weakening friction,[16] and some corresponding models have been proposed[21,22] which also show slipping events spanning a wide range of event sizes in a wide range of parameter values.

The equations of motion (5) are coupled differential equations and were solved numerically by use of the standard Runge–Kutta procedure. We mainly studied systems with size $N = 50$. Calculations in larger systems with size up to $N = 150$ were also performed to verify that scaling and the other dynamic behavior obtained are not a finite-size effect and to study the size dependence of the system's fracture energy.

The system was always started completely at rest from a spatial configuration of eq 7 or eq 8. There was then a transient period before the system reached a steady state, at which point data for the calculations were collected. The motion of the system is in general not periodic either in time or in space. In the steady state, large slipping events, which involve a large part of the system, however, appear to be approximately periodic in time. This big-event period (loading period) is proportional to $k/v$ and in our calculations ranges from 80 to 200. The system reaches its steady state in about 10 loading periods, and we typically discarded the data of the first 15 periods. The time steps used in the numerical procedure were $10^{-4}$ of the loading period. Typically data from 500 cycles, or about $5 \times 10^6$ time steps, were used for the calculations.

## 3. Stick-Slip Dynamics

**Time and Space Distributions.** As the chain is pulled, the external pulling force adds potential energy to the system. The high-barrier sections of the random Gaussian potential represent tight entanglements and tend to keep particles at these locations from moving, while particles at low potential barriers move easily through loose entanglements when there is a small stress. This creates small slipping events which involve a small number of particles and have small magnitudes of slipping. Eventually, after a long enough time for there to be enough stress accumulated in the system, the particles in the deepest potential wells will move. This will then trigger motion involving a large number of particles and large magnitudes of slipping, and the system exhibits large dynamic events.

A dynamic event is defined[22] as a collection of motions of particles that are all connected in time and space. The moment $M$ of an event, which is used to measure the size of the event, is defined as the total displacement in the event,

$$M = \sum_i \delta x_i \quad (9)$$

where $i$ is summed over all particles involved in the event. A more frequently used quantity for measuring the size of an event is the magnitude $\mu$ of the event, defined as the logarithm of $M$,

$$\mu = \ln M \quad (10)$$

The event probability distribution $P(\mu)$ is the frequency of events per unit interval of $\mu$. It is of particular interest since seismological data[24] and some earthquake models[17,19,22] show that $P(\mu)$ obeys a scaling law for small- and medium-magnitude earthquakes of the form

$$P(\mu) = Ae^{-b\mu} \quad (11)$$

with $b \approx -1$, where $A$ is a constant. It is clearly of importance to known whether a similar distribution of event sizes will occur in the case of polymer chain pull-out, since the energy required for fracture will depend on

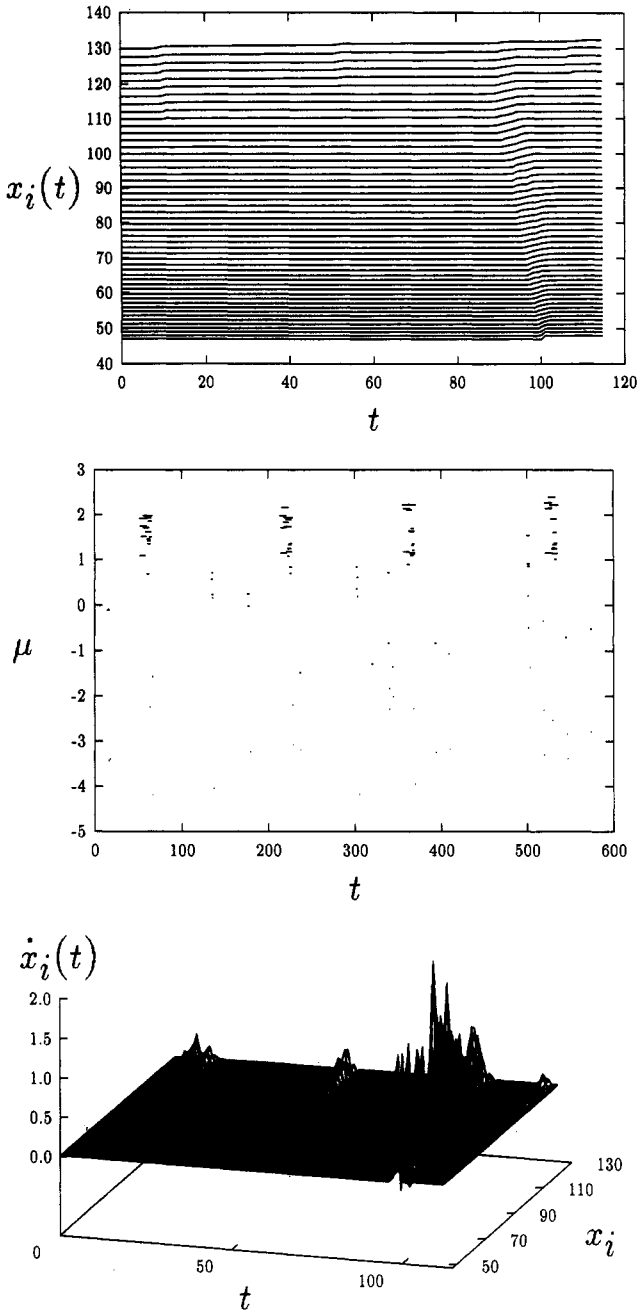


**Figure 2.** Demonstrations of the stick–slip dynamics for the model. A wide range of slipping events are shown from different points of view, but for the same parameters: $s_1 = 60$, $s_2 = 20$, $k = 220$, $v = 0.015$, and $\gamma = 3.0$. (a) Displacement of blocks as a function of time. (b) Time distribution of events, showing clustering of events in time, and an approximate periodic distribution of large events. (c) The velocities of the blocks are shown as a function of position and time. Both big, global and small, localized events are seen.

this distribution. We will accordingly seek to determine the form of $P(\mu)$. For simplicity we work in terms of a normalized $P(\mu)$ obtained by dividing the number of events per unit $\mu$ interval by the total number of events in the entire run.

We first look at the spatiotemporal dynamics of the chain pull-out process. The stick–slip dynamics of a wide range of event magnitudes was observed as the chain was pulled out. The dynamics can be seen from the plot of particle displacements $x_i(t)$ as a function of time in a chain of 50 particles, as shown in Figure 2a. For most of the time, most particles are in a stuck state, which is indicated in the figure by smooth, horizontal lines. Also seen in the figure are small slipping events, which are indicated by sudden jumps in position of a cluster of particles, and large events indicated by large displacements in which a large number of particles are involved. One time unit in the figure is 67 time steps. The fact that the lines are more widely spaced for large $i$ than for small $i$ is due to the relatively greater tension in the end of the chain that is being pulled.

Figure 2b shows the time distribution of events and event magnitudes. A horizontal bar indicates an event and its magnitude, and the length of the bar gives the total time duration of the event. A larger event usually has a longer time duration. We first see that a wide range of magnitudes of events is observed: the event size (moment) spans over 3 orders of magnitude. Events are not periodic in time, but they tend to form clusters in time. Since one large or several mid-size events will release most of the accumulated stress in the system, there is a relatively quiet period between two clusters of events, during which the stress again accumulates.

An alternative method of presenting the data is to plot the velocities of the particles as a function of position and time. As shown in Figure 2c, which shows data for a model having the same parameters as parts a and b of Figure 2, both a large event, involving the whole system, and relatively small events are observed in the time period presented. The former is characterized by high and global peaks of velocities which are much greater than the pulling speed, and the latter, by low and localized peaks of velocities. Very small events with velocities on the order of the pulling speed cannot be seen in the figure at the scale used. The presence of very small events is better seen in the event probability distribution $P(\mu)$ to be discussed in the next section.

The spatiotemporal dynamics in the chain pull-out process described above appears similar in some ways to that in some spring–block earthquake models[19–22] in which every block is pulled at the same constant speed. However, the absence of the pulling force on every particle except one in the present model does cause some differences in the dynamic behavior of the system both quantitatively and qualitatively. Although the time distribution in Figure 2b shows that large events form clusters and distribute quasi-periodically in time, as is the case in spring–block earthquake models, the period in the present model does not depend on the pulling spring parameter $s_2$ because there is now only the end particle that is pulled, while in the earthquake models the interval between major events is proportional to $k/(vs_2)$. The intervals in this model are greater than those in the earthquake models when the other parameters are the same because the single $s_2$ spring in the chain can be thought of as acting in a similar way to a large number of small $s_2$ in the case where every particle is pulled.

Another significant effect of having the chain pulled by a force applied to only the one particle at the end of the chain is that the system will never lose its instability. In the model[22] where every particle is pulled, it was found that substantially increasing $s_2$ leads the system into a state where there are only creeping motions and no large events. We used a range of values of $s_2$ up to 400 and found the system still to show stick–slip dynamics, whereas in ref 22 an $s_2$ of 100 led the system to lose its instability. The single pulling force on the chain also affects the scaling behavior of the event magnitude distribution as is discussed below.

**Scaling of the Magnitude Distribution.** Our goal is to understand the effect of changing such parameters as bond elasticity and strength of interchain interaction on

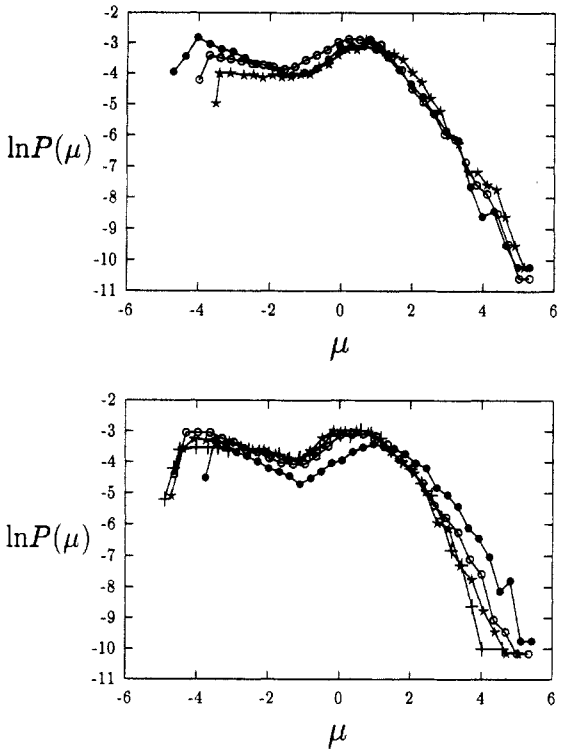


**Figure 3.** Logarithm of event probability distribution $P(\mu)$ as a function of event magnitude $\mu$. Two parameters in the model can change the scaling of the distribution in the small-event region ($\mu < \mu_0$): (a) a stronger dissipation $\gamma$ yields a smaller scaling exponent $b$ (in eq 11). Parameters are $s_1 = s_2 = 100$, $k = 250$, $v = 0.015$, and $\gamma = 3.0$, 3.8, and 5.0 for curves with filled circles, open circles, and stars, respectively; (b) a smaller parameter $s_1$ gives a larger exponent $b$. Here $s_1$ is 60, 100, 150, and 200 for the filled circle, open circle, star, and plus curves respectively, and the other parameters are $s_2 = 20$, $k = 250$, $v = 3.0$, and $\gamma = 3.0$.

the fracture energy. In order to achieve this, we need to know how the event magnitude distribution depends on these variables, since it is this function that provides a quantitative measure of the character of the stick–slip dynamics. It is an important measurement also because of its connection with universality: the existence of the same distribution exponent for various different systems suggests that they obey the same scaling law for equivalent quantities, even though their origins and physical meanings may be different. We calculated the function $P(\mu)$ for various different parameter values and measured the scaling exponent $b$ in eq 11 for small and medium events. These slipping events account for the majority of the slipping events that occur, and hence the scaling of their distribution is important in attaining an accurate statistical picture of the dynamics. Figure 3a shows the distribution $P(\mu)$ for three different values of dissipation constant $\gamma$. As a characterization of the stick–slip dynamics, $P(\mu)$ again shows the wide range of event size of the dynamics: events with moments spanning over 3 orders of magnitude were recorded. The crossover magnitude $\mu_0$ in the figure divides the distribution into small-event and large-event regions. We will only study the scaling behavior of the small- and medium-event regions in this paper. The distribution in the large-event regime does not seem to fit eq 11 with a constant exponent $b$. The parameters in Figure 3a are $s_1 = s_2 = 100$, $k = 250$, $v = 0.015$, $\gamma = 3.0$ for the curve with filled circles, $\gamma = 3.8$ for the curve with open circles, and $\gamma = 5.0$ for the curve with stars. The scaling exponents $b$ for these three cases are approximately $b = 1.0$, 0.5, and 0.1, respectively. We see that a stronger dissipation yields a smaller exponent $b$. This indicates that a stronger dissipation depresses small slipping events and causes the motion of the system to be more dominated by intermediate-size and large events. This dependence of the scaling exponent on dissipation is similar to that found in our previous model[22] and in some macroscopic experiments.[16]

One difference between the present single-pulling-force model and our previous model is the sensitive dependence of $b$ on the interparticle interaction parameter $s_1$. In our previous model varying $s_1$ had almost no effect on the exponent $b$ within the wide range that we studied. Figure 3b, on the other hand, shows the effect of $s_1$ on $b$, where $s_2 = 20$, $k = 250$, $v = 0.015$, $\gamma = 3.0$, and $s_1 = 60$, 100, 150, and 200 for filled circles, open circle, star, and plus curves, respectively. A smaller $s_1$ yields a higher probability of very large events but fewer small- and intermediate-size events. A larger $s_1$ flattens the distribution in the small-event region, which indicates that a stronger interparticle interaction suppresses small events. We also note that the distribution has a large change as $s_1$ is changed from 60 to 100 but smaller changes after $s_1 > 100$. We will see a similar dependence of fracture energy on $s_1$ later.

The parameter $s_2$ has virtually no effect on the distribution $P(\mu)$ because it acts only on a single particle at the end of the chain. We calculated two distributions $P(\mu)$ for $s_2 = 20$ and 100 with the same parameters $s_1 = 100$, $k = 250$, $v = 0.015$, and $\gamma = 3.0$ and found the two resulting distributions to be identical. Although $s_2$ did not have a perceptible effect on the dynamics of chain pull-out for the range of parameters studied, we do note that, as $s_1$ becomes sufficiently large that local events are suppressed, the effect of $s_2$ must become more important.

The potential-depth parameter $k$ affects the distribution $P(\mu)$ but does not change the scaling exponent $b$. A larger $k$ induces more large events and thus moves the $P(\mu)$ curve to the right for large $\mu$ but does not alter the distribution of small events. Figure 4a shows the effect of $k$ on the event magnitude distribution.

Changes in pulling speed $v$ also do not change the scaling exponent $b$. Shown in Figure 4b is the distribution $P(\mu)$ at two $v$ values with other parameters fixed. While the two distributions have the same scaling, they differ from each other in other ways. The system has more of the very smallest events at small pulling speeds, as is indicated by the extended distribution in the small-$\mu$ region. A larger speed $v$, on the other hand, induces more intermediate events.

In our calculations we set a criterion for a minimum displacement $\Delta x_{min}$ that could be counted as a measured event. Any event with a displacement (in a given time interval) smaller than $\Delta x_{min}$ was ignored. This criterion is necessary to exclude measurement or calculation noise from the recorded events in experiments and computations. We have set $\Delta x_{min}$ to be the distance traveled at twice the pulling speed $v$ in one time step $\Delta t$,

$$\Delta x_{min} = 2v\Delta t \tag{12}$$

This $\Delta x_{min}$ is arbitrary. If it is set to a small value or to zero, as was the case in ref 19, the distribution $P(\mu)$ will extend in the small $\mu$ direction with the same scaling. This indicates that small-magnitude events are much more frequent than large events. It has been shown in our previous work that changing $\Delta x_{min}$ does not change the scaling exponent $b$.

The ability of the chains in the polymer matrix to deflect as the pulled chain passes them is the basis for the viscosity characterized by the dissipation parameter $\gamma$. We might expect a very flexible system to deform readily under stress and that small stick–slip motion would be less frequent.

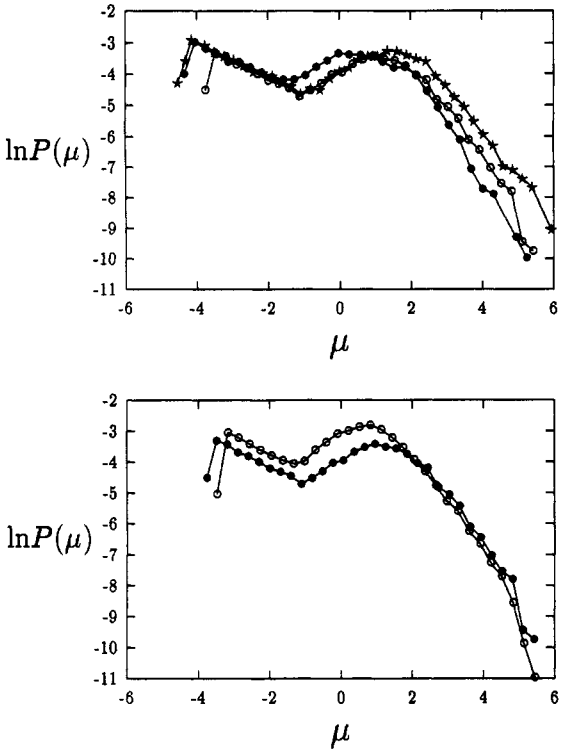


**Figure 4.** Scaling exponent $b$ of the distribution $P(\mu)$ is not affected by changes in the other parameters in the model, although the distribution itself can be altered. (a) The effect of larger $k$ is to induce more very large events. The three curves correspond to $k$ = 150 (filled circles), $k$ = 250 (open circles), and $k$ = 350 (stars). All three curves have $s_1$ = 60, $s_2$ = 20, $v$ = 0.015, and $\gamma$ = 3.0. (b) A system with a larger pulling speed ($v$ = 0.03, open circles) also has a larger probability for medium-magnitude events compared to that with a smaller pulling speed ($v$ = 0.015, filled circles). Here $s_1$ = 60, $s_2$ = 20, $k$ = 250, and $\gamma$ = 3.0.

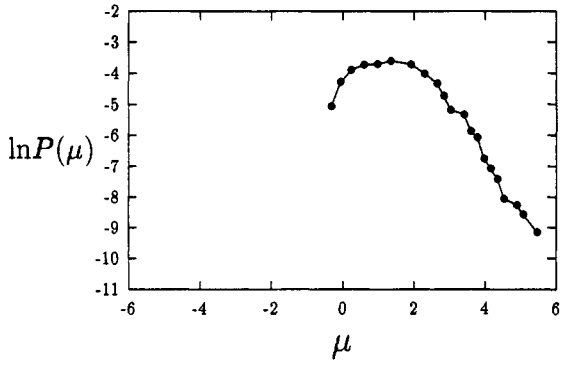


**Figure 5.** The system changes to the state where only large events are seen when the dissipation $\gamma$ and potential depth $k$ are large. This transition is continuous as $\gamma$ and $k$ are increased. Shown here is a system with $s_1$ = 60, $s_2$ = 20, $v$ = 0.015, $k$ = 300, and $\gamma$ = 5.0.

This is indeed the case. As the dissipation $\gamma$ is increased, small events are suppressed or become too small (less than $\Delta x_{min}$) to be detected. The system dynamics will then have no small events and be dominated by stuck and large slipping motions. This type of dynamics can be seen in Figure 5 where the distribution starts at some intermediate value of event magnitude $\mu$, approximately equal to the crossover value $\mu_0$. The change from the dynamics of a wide range of event magnitudes to that of only large events is continuous as the dissipation is increased.

To verify that the stick–slip dynamics described above does not depend on the size of the system studied, we have calculated the distribution $P(\mu)$ for systems with size $N$ = 100 and 150. The (normalized) distributions $P(\mu)$ calculated from these larger systems are almost identical to that from the system of $N$ = 50. This shows the independence of the stick–slip dynamics of this model on the system size.

Finally, as a check on whether the surface of the polymer matrix was an active factor in determining the dynamic behavior, we calculated $P(\mu)$ for a chain that did not emerge from the matrix but instead formed a closed loop within the polymer host. This system had periodic boundary conditions, and so surface effects were eliminated. We found that the exponent $b$ was unchanged by the use of periodic boundary conditions but that the system then had fewer large events and more small events than the comparable system with open boundary conditions. The motion in a periodic boundary system thus is much quieter than that in an open-boundary system but has the same qualitative form.

## 4. Fracture Energy

We next calculated the energy needed to pull out a polymer chain from the matrix in which it is embedded. Since this model only considers the fracture mechanism where one of the shorter diblock copolymer chains is pulled out from the corresponding homopolymer matrix, the only energy-consuming mechanism is the energy dissipation from the viscous pull-out of the chain.[3] We accordingly computed the energy $G$ per chain that is consumed by viscosity during the pull-out process,

$$G = \sum_{\Delta t}\sum_{i} \gamma \dot{x}_i^2 \Delta t \tag{13}$$

where $\Delta t$ is the time step used in the numerical procedure and is summed through the entire pull-out process, and $i$ is summed over all particles. We investigate the dependence of $G$ on chain length $N$, chain elastic parameter $s_1$, roughness of interface between the matrix and the chain $k$, the coefficient of viscous dissipation $\gamma$, and the pulling speed $v$. In general, we found $G$ to be a function of all these parameters.

The critical fracture energy $G_c$ is the minimum energy required to break the interface between the homopolymer and the diblock copolymer. To calculate $G_c$, we first verified that $G$ is a slowly varying function of $v$ for small $v$ and then used a very small pulling speed and a range of other parameters to determine $G_c$. We used the same speed for all calculations of $G_c$. The $G_c(N)$ obey a power law of the form $G_c \propto N^\alpha$ reasonably well but with an exponent $\alpha$ that is a function of $k$ and $s_1$. As mentioned earlier, contradictory forms of the power-law dependence of $G_c$ on $N$ have been obtained in some theoretical models, where both $\alpha$ = 1 and $\alpha$ = 2 were predicted, while the results from experiments are somewhat ambiguous. Figure 6 shows the form we find for the $N$ dependence of $G_c$ with $s_1$ = 60 and $k$ = 150, $s_1$ = 100 and $k$ = 150, and $s_1$ = 100 and $k$ = 50 from top to bottom, respectively. The solid line shows the power-law fit to the first curve. The exponent $\alpha$ for the three curves shown are, from top to bottom, 1.86, 1.77, and 1.52, respectively. We see from the figure that $G_c$ increases when one increases the strength of the interchain interaction $k$ but decreases when one increases the strength of the intrachain spring constant $s_1$. This can be understood when we look at the effects to $k$ and $s_1$ on the dynamics of the pull-out process. A large $k$ gives larger static friction since the interface between the chain and the matrix is rougher, and so a larger elastic energy is required in order for particles to start slipping. Once the particles overcome the matrix background

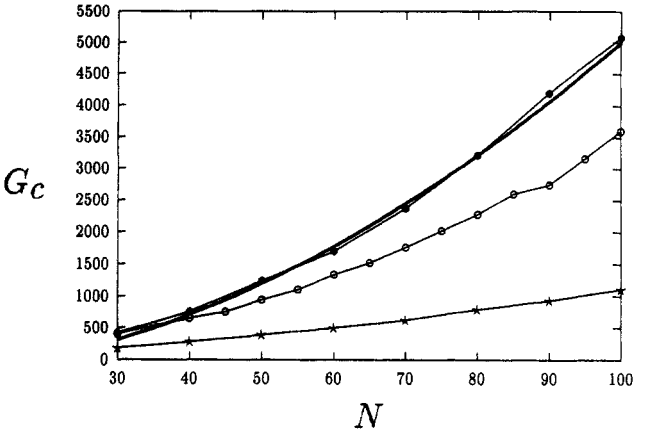


**Figure 6.** Critical fracture energy $G_c$ as a function of chain length $N$. Note that $G_c$ is also a function of the parameters $s_1$ and $k$. The top curve is for the system with $s_1 = 60$ and $k = 150$ (the heavy line is a power-law fit with an exponent of 1.86), the middle one with $s_1 = 100$ and $k = 150$, and the bottom one with $s_1 = 100$ and $k = 50$. The two lower curves obey the power law with exponents of 1.77 and 1.52, respectively.

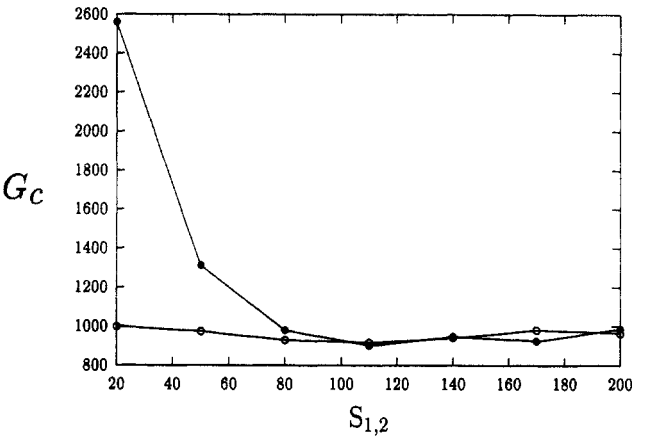


**Figure 7.** $s_1$ and $s_2$ dependences of $G_c$. The parameters are $k = 150$, $v = 0.015$, and $\gamma = 3.0$. For the $s_1$ curve (with filled circles) $s_2 = 100$, and for the $s_2$ curve (with open circles) $s_1 = 100$.

potential and start to move, the larger stored energy will generate larger slipping velocities, which in turn will consume more energy. Also, as we have seen before, a small $s_1$ induces more large events. Since large events involve large velocities and a large number of particles, a smaller $s_1$, hence softer chains, will thus dissipate more viscous energy.

Since $s_1$ is an elastic parameter of the polymer chain and $k$ is the interaction parameter between the chain and the matrix, the dependence of $G_c$ on $s_1$ and $k$ indicates that the critical fracture energy depends both on the type of chain being pulled out and on the type of matrix in which the chain is embedded, in addition to being a function of the chain length.

We have seen in Figure 6 that the critical fracture energy $G_c$ is a decreasing function of $s_1$ and an increasing function of $k$. To see clearly the dependence of $G_c$ on the chain spring constant $s_1$, we fixed all other parameters and calculated $G_c$ for different $s_1$, as shown in Figure 7. We see that $G_c$ is strongly dependent on $s_1$ when $s_1 \leq 80$ but becomes almost independent of it when $s_1 \geq 80$. We recall that a similar dependence on $s_1$ of the event distribution $P(\mu)$ was observed in Figure 3b. This is another example showing that the dynamics of the pull-out process is closely related to the fracture energy during the process. Also shown in Figure 7 is $G_c$ as a function of $s_2$ with all other parameters fixed. Again we see that changing $s_2$ has

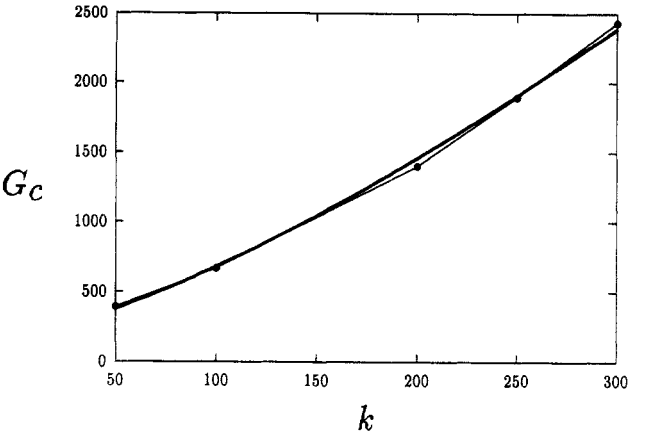


**Figure 8.** Dependence of $G_c$ on the maximum-depth parameter $k$ of the potential. The solid line is the power-law fit with a power of 1.35.

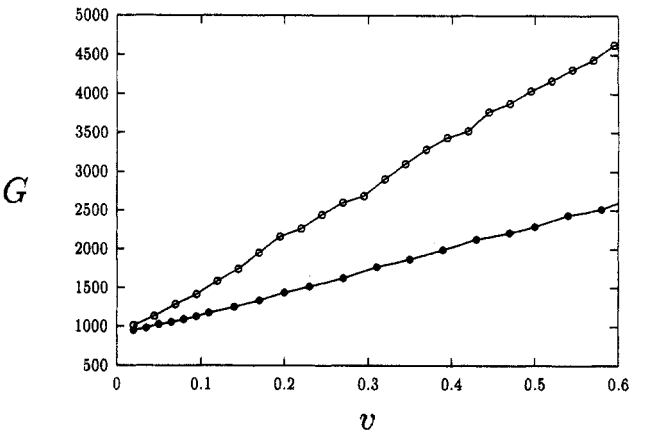


**Figure 9.** Fracture energy $G$ as a function of pulling speed $v$. A good linear relationship between them was obtained in this speed range. The two curves correspond to two different dissipation levels with $\gamma = 6$ for the top curve and $\gamma = 3$ for the bottom curve.

virtually no effect on $G_c$. This is reminiscent of the dynamic behavior we have seen before.

Figure 8 shows the relationship between $G_c$ and the strength of the interaction $k$ between the chain and the matrix when the other parameters, $s_1$ and $s_2 = 100$, $v = 0.015$, and $\gamma = 3.0$, are kept unchanged. The best power-law fit to the relationship is $G_c \sim k^{1.35}$ for the parameter set chosen, but again the exponent is not universal, depending on $s_1$, $v$, and $\gamma$. It is, however, always positive.

The pulling speed $v$ in this model is not directly the crack propagation speed measured in experiments. It is, however, approximately proportional to the crack speed if the interface is separated by peeling at a constant speed as was done in ref 3. Two fracture energies $G$ are plotted in Figure 9 as a function of pulling speed $v$ for two different dissipation coefficients $\gamma$. The figure shows that $G$ increases linearly with $v$ for $v < 0.6$. This result differs from that of previous theoretical models[10-12] in that we did not obtain any predicted critical velocity $v^*$ below which $G$ is a constant independent of crack speed. However, we note that there is as yet no clear experimental evidence for the existence of any critical $v^*$. Figure 9 also shows that a larger dissipation coefficient results in a larger energy consumption during the chain pull-out process, even though the slipping velocities are thereby reduced.

The dependence of the fracture energy $G$ on the pulling speed $v$ is also related to the dynamic effects of $v$ on the system. Although, as we have seen earlier, changing $v$ does not change the scaling of the event distribution $P(\mu)$,

a larger $v$ does nevertheless induce more intermediate and large events, which have high slipping velocities and thus produce higher viscous energy dissipation.

The linear relation between $G$ and $v$ is maintained up to about $v \sim 0.8$, after which there is a decrease in slope of the curve. While we did not find the experimentally observed total saturation of $G(v)$ after some critical value of $v$, our results are somewhat closer to experiment than the dependence of $G$ on $v$ predicted by some theoretical models.[10-12]

As was the case for $G_c$, we find that $G$ is also a function of the other parameters. Small $s_1$, large $k$, or long chain length $N$ all cause an increase in $G$.

## 5. Conclusions and Discussion

We have proposed and studied a one-dimensional microscopic mechanical model for the interface fracture process that occurs when diblock copolymer chains are pulled out from a homopolymer matrix. This model has been applied to the chain pull-out process in glassy polymers but should be applicable to elastomers as long as the pull-out rate is small and the chains are short. The chain pull-out from glassy polymers has been observed in PS–PVP[3] and PS–PMMA[8] systems. The chain pull-out from elastomers has been reported in ethylene–propylene–diene terpolymer and poly(isobutylene-*co*-isoprene)[6] and PS–PI systems.[2,7] We have studied the spatiotemporal dynamics of the model and have observed stick–slip behavior displaying various slipping events with a wide range of magnitudes. These dynamics have many of the characteristics of self-organized critical systems and thus resemble the situation encountered when grains of sand are dropped continuously onto the top of an accumulating sand pile. In just the same way as the slope of the sand pile adjusts itself to be at the critical value at which avalanches occur, the polymer chain being pulled from the matrix repeatedly undergoes avalanche-like motion in which large chain segments break loose from the trapping potential. This type of behavior has been observed in our calculations for a wide range of model parameters. The scaling behavior of the event probability distribution $P(\mu)$ for small slipping events was calculated and found to change with the dissipation constant and with the chain stiffness. Other model parameters, although changing the distribution in some ways, do not change the scaling. The fact that the pulling force acts only on the end particle in our model has some special effects which distinguish the dynamics of this system from that of models of earthquake dynamics, in which every particle is pulled equally. The model also seems to be a robust system for self-organized slipping in that the characteristic spatiotemporal dynamics do not depend on the size of the system, boundary conditions, initial configurations, or pulling speed.

We have also calculated the fracture energy $G$ of pulling out a single chain from the matrix. The critical energy $G_c$, below which no pull-out occurs, and its dependence on chain length, chain elastic parameter, roughness of interface between the chain and the matrix, and level of dissipation were also studied. We found that, in general, the $G_c$ is a function of all the above parameters but that there is a power-law relationship between $G_c$ and $N$ in which the exponent depends on the other parameters of the chain and on the nature of the interface between the pulled chain and the matrix. A linear dependence of fracture energy $G$ on pulling speed $v$ is maintained for modest values of $v$ but then partially flattens out. This linear relationship between $G$ and $v$ emerges from the calculations for our microscopic model and is not an assumption of the type used in some theoretical models. The complete saturation observed in experiments was, however, not observed in our simulations. It is possible that this saturation could be related to the phenomenon of chain scission, which was not included as an ingredient in our model.

**Acknowledgment.** This work was supported by the National Science Foundation Materials Research Group Program under Grant No. DMR91-22227 and made use of the resources of the Ohio Supercomputing Center. We thank Dr. A. M. Jamieson for his helpful comments on the manuscript.

## References and Notes

(1) Present address: Department of Physics, University of Minnesota, Minneapolis, MN 55455.
(2) Brown, H. R. *Macromolecules* **1993**, *26*, 1666.
(3) Creton, C.; Kramer, E. J.; Hui, C. Y.; Brown, H. R. *Macromolecules* **1992**, *25*, 3075.
(4) Creton, C.; Kramer, E. J.; Hadziioannou, G. *Macromolecules* **1991**, *24*, 1846.
(5) Washiyama, J.; Kramer, E. J.; Hui, C. Y. *Macromolecules* **1993**, *26*, 2928.
(6) Ellul, M. D.; Gent, A. N. *J. Polym. Sci., Polym. Phys. Ed.* **1985**, *23*, 1823. Ellul, M. D.; Gent, A. N. *J. Polym. Sci., Polym. Phys. Ed.* **1984**, *22*, 1953.
(7) Brown, H. R.; Reichert, W. F. *Macromol. Rep. A* **1992**, *29* (supp. 2), 201. Reichert, W. F.; Brown, H. R. *Polymer* **1993**, *34*, 2289.
(8) Brown, H. R.; Char, K.; Deline, V. R. *Macromolecules* **1993**, *26*, 4155.
(9) Char, K.; Brown, H. R.; Deline, V. R. *Macromolecules* **1993**, *26*, 4164.
(10) de Gennes, P.-G. *Can. J. Phys.* **1990**, *68*, 1049.
(11) Raphaël, E.; de Gennes, P.-G. *J. Phys. Chem.* **1992**, *96*, 4002.
(12) Xu, D. B.; Hui, C. Y.; Kramer, E. J.; Creton, C. *Mech. Mater.* **1991**, *11*, 257.
(13) Ji, H.; de Gennes, P.-G. *Macromolecules* **1993**, *26*, 520.
(14) Tullis, T. E.; Weeks, J. D. *Pure Appl. Geophys.* **1986**, *124*, 383.
(15) Feder, H. J. S.; Feder, J. *Phys. Rev. Lett.* **1991**, *66*, 2669.
(16) Vallette, D. P.; Gollub, J. P. *Phys. Rev. E* **1993**, *47*, 820.
(17) Burridge, R.; Knopoff, L. *Bull. Seismol. Soc. Am.* **1967**, *57*, 341.
(18) Takayasu, H.; Matsuzaki, M. *Phys. Lett. A* **1988**, *131*, 244. Matsuzaki, M.; Takayasu, H. *J. Geophys. Res.* **1991**, *96*, 19925.
(19) Carlson, J. M.; Langer, J. S. *Phys. Rev. Lett.* **1989**, *62*, 2632. Carlson, J. M.; Langer, J. S. *Phys. Rev. A* **1989**, *40*, 6470.
(20) Vasconcelos, G. L.; de Sousa Vieira, M.; Nagel, S. R. *Physica A* **1992**, *191*, 69.
(21) Knopoff, L.; Landoni, J. A.; Abinante, M. S. *Phys. Rev. A* **1992**, *46*, 7445.
(22) Lin, B.; Taylor, P. L. A model of spatiotemporal dynamics of stick-slip motion. *Phys. Rev. E*, in press.
(23) Bak, P.; Tang, C.; Wiesenfeld, K. *Phys. Rev. Lett.* **1987**, *59*, 381.
(24) Guterberg, B.; Richter, C. F. *Ann. Geofis.* **1956**, *9*, 1.